Asian Journal of Chemistry; Vol. 27, No. 6 (2015), 2209-2216

ASIAN JOURNAL OF CHEMISTRY

http://dx.doi.org/10.14233/ajchem.2015.18086

Synthesis, Characterization and Antimicrobial Activity of Triazamacrocyclic Based Polymeric Ligand and its Polymer-Metal Complexes

SAAD M. ALSHEHRI*, EIDA AL-FARRAJ, NORAH ALHOKBANY and TANSIR AHAMAD

Department of Chemistry, King Saud University, Riyadh, Kingdom of Saudi Arabia

*Corresponding author: Fax: +966 114674018; Tel: +966 114675971; E-mail: alshehri@ksu.edu.sa; ahamed@ksu.edu.sa

Received: 27 May 2014; *Accepted*: 9 December 2014; *Published online*: 17 March 2015; AJC-16995

A triazamacrocyclic-based polymeric ligand (poly-H_3L) was synthesized *via* polycondensation of 1,4,7-triazacyclonone-1,4,7-tripropionic acid (NOTPA) and ethylenediamine and polymer-metal complexes were prepared with Cu(II), Zn(II), In(III) and Ga(III) ions. All of the synthesized polymers were characterized by elemental, spectral and thermal analyses. The elemental and spectral data revealed that the poly-HLM(II) are five-coordinate complexes in which the metals are coordinated to three nitrogen atoms in the macrocycle and are coordinate covalently bound to two amide groups. However, the poly-LM(III) are six-coordinate complexes. The thermal kinetics, such as the activation energy and the thermodynamic parameters of the synthesized polymers were evaluated during pyrolysis using the Coats-Redfern equation. In addition, the antimicrobial activity of the synthesized polymers was evaluated against several microorganisms using agar-well diffusion methods. Among all of the polymer-metal complexes, the antimicrobial activity of the Cu(II)-chelated polymer exhibited the largest zone of inhibition.

Keywords: NOTA, Polycondensation, Polymer-metal complexes, FT-IR, Activation energy, Antimicrobial activity.

INTRODUCTION

Transition-metal complexes are one of the most important and commonly used classes of compounds in various industrial and biological fields due to their good cost/performance ratio[1,2]. However, one of the drawbacks associated with these compounds is their poor stability and flexibility. In contrast, metal-containing polymers are more stable and impart flexibility because of their organic moiety. They also exhibit high stability due to the presence of inorganic functional groups in the same polymeric backbone[3-5]. These properties make metal-containing polymers highly useful in industrial and scientific applications. Previously, a number of polymer-metal complexes have been prepared and reported[6-10]. These polymer-metal complexes were screened against several microorganisms to examine their antimicrobial and antifungal activities. The results indicate that these polymer-metal complexes were exhibit superior antimicrobial activities then those of the polymeric ligands alone.

The macrocyclic complexes have been observed to be more stable than linear monodentate or polydentate ligands[11]. Numerous macrocyclic ligands are known. However, the coordination chemistry of many transition-metal ions with N-substituted tri-aza and tetra-aza macrocyclic ligands, such as NOTA and DOTA, are currently being investigated for a number of applications in such fields as analytical chemistry, biochemistry and medicine[12-14]. They are also used as mimics for enzymes, such as in models of photosystem II production. NOTA and DOTA have been utilized in MRI and photometric or radioactive imaging and therapy because these compounds form the same molecule, a chelating group and a chemically reactive functional group, which can be covalently attached to macromolecules or polymers[15-18]. A literature survey indicate that few studies have been reported on the NOTA-based polymeric ligand and its polymer-metal complexes. Here, we report the synthesis, characterization and antimicrobial activities of a triazamacrocyclic-based polymeric ligand and its polymer-metal complexes with Cu(II), Zn(II), In(III) and Ga(III) ions. The antimicrobial activity of these polymers was tested against several bacteria and fungi using agar-well diffusion methods.

EXPERIMENTAL

1,4,7-Triazacyclonoanane, ethylenediamine, sodium hydroxide and Cu(II), Zn(II), In(III) and Ga(III) chlorides (Sigma-Aldrich) were used without further purification. Solvents such as acetone, methanol, ethanol, diethyl ether, tetrahydrofuran (THF), dimethylformamide (DMF) and dimethylsulfoxide (DMSO) were purified *via* standard procedures before use. Tryptic soy agar (TSA) and tryptic soy broth (TSB) were purchased from Difco Laboratories. All the strains used for the antimicrobial activity studies were acquired

from the microbiology research laboratory at King Saud University. NOTPA was prepared according to a previously reported method[19]. The elemental analyses of the synthesized polymeric compounds were performed on a Perkin Elmer model 2400 elemental analyzer. The FTIR spectra were recorded from 4000 to 400 cm^{-1} on a Bruker Tensor-27 spectrophotometer; the samples for FTIR were prepared in KBr pellets. Thermogravimetric (TG) experiments were performed using simultaneous thermogravimetry (TA Instruments STD 600). ^1H NMR and ^{13}C NMR spectra were recorded on a JEOL-GSX 400-MHz FT-NMR spectrometer using DMSO-d_6 as a solvent and tetramethyl silane (TMS) as an internal standard. The UV-visible spectra were collected on a Shimadzu spectrophotometer (UV-1650 PC) using DMSO as the solvent. Gel permeation chromatography was performed on a Polymer Laboratories GPC220 instrument with tetrahydrofuran as the solvent and polystyrene as a standard. Thermal behaviours, thermal kinetics and thermodynamic parameters of each synthesized polymer were recorded on a SDT Q-600 simultaneous thermogravimetric analyzer and differential scanning calorimeter (TA Instruments) under a nitrogen atmosphere at a heating rate of 5, 10, 15 or 20 °C min^{-1}.

Antibacterial activity: The antibacterial activity of the polymeric ligand and its polymer-metal complexes was analyzed against *B. subtilis*, *B. megaterium*, *S. aureus*, *E. coli*, *P. aeruginosa* and *S. typhi*. All of the synthesized polymers were dissolved in DMSO separately during the preparation of 50 µg/mL solutions. Bacterial strains were nourished in a nutrient broth (Difco) and incubated on Mueller-Hinton agar for 24 h. Wells were carved into the media using a sterile steel borer and 0.1 mL of each sample was subsequently introduced into the corresponding well. The Petri dishes were incubated at 37 °C and the inhibition zones were measured (in mm) after 24 h of incubation. Each experiment was repeated three times. The antibacterial activity of the solvent (DMSO) and a common standard antibiotic, kanamycin, were also recorded as positive and negative controls, respectively.

Antifungal activity: The antifungal activity of the synthesized polymers, the blank (DMSO solvent) and the standard drug miconazole were tested against various fungi, *viz*., *C. albicans*, *T. species*, *A. flavus*, *A. niger*, *F. species* and *M. species*. DMSO solutions of each compound were prepared at a concentration of 100 µg/mL. The fungus strains were nourished in a malt extract broth (Difco) and were incubated for 48 h on Sabouraud dextrose agar. The wells were carved into the media using a sterile steel borer and 0.1 mL of each sample was subsequently introduced into the corresponding well. The other wells were supplemented with solvent (DMSO) as the positive control and the standard drug miconazole as the negative control. The Petri dishes were incubated at 30 °C and the inhibition zones were measured (in mm) after 72 h of incubation.

Synthesis of the NOTPA: NOTPA was prepared by the reaction of 1,4,7-triazacyclonoanane (TACN) (1 mmol, 0.10 g) and acrylic acid (3 mmol, 0.16 g) in acetone (30 mL), the reaction mixture was stirred at room temperature for 2 h to give a yellowish precipitate. The resulting precipitate was filtered and washed with diethyl ether and ethanol and dried in a vacuum oven to give a light yellow powder in 80 % yield (0.27 g). FTIR (KBr, ν_{max}, cm^{-1}): 3411, 3231, 2935, 2845, 2350, 1751, 1654, 1402, 1240, 621; ^1H NMR (400 MHz, DMSO, δ): 12.02 (s, 3H, O<u>H</u>), 3.62 (s, 6H, -CH_2-C<u>H_2</u>-C=O), 3.02 (s, 6H, N-C<u>H_2</u>-CH_2-C=O), 2.36 (t, 12H, N-C<u>H_2</u>-C<u>H_2</u>-N): ^{13}C NMR (100 MHz, DMSO, δ) 172.80, 60.83, 52.12, 35.65 ppm; Anal. $C_{15}H_{27}N_3O_6$ (345.0): Calc: C, 52.17; H, 7.82; N, 12.17; found: C, 52.08; H, 7.70; N, 12.04 % .

Synthesis of the NOTPA-based polymeric ligand [poly-H_3L]: In a 250 mL round-bottom flask, NOTPA (0.345 g, 0.001 mol) was dissolved in 30 mL of ethanol and ethylenediamine (0.198 mL, 0.003 mol) was added and the solution was then mixed at room temperature. The mixture was refluxed with continuous stirring at 80 °C for 5 h and the progress of the reaction was monitored by thin-layer chromatography (TLC). The solvents were removed under reduced pressure with a rotary evaporator. The resulting light-gray-coloured, viscous product was washed with diethyl ether and ethanol and dried in a vacuum oven to remove any trapped solvents to yield the NOTPA-based polymeric ligand [poly-H_3L] in 73 % yield. FTIR (KBr, ν_{max}, cm^{-1}): 3425, 2956, 2840, 1680, 1475, 1460, 1387, 1190, 860, 703; ^1H NMR (400 MHz, DMSO, δ): 8.14 (s, 3H, N<u>H</u>), 3.35 (t, 6H, NH-C<u>H_2</u>-C<u>H_2</u>), 2.84 (t, 6H, N-C<u>H_2</u>-CH_2-), 2.45 (t, 6H, -CH_2-C<u>H_2</u>-C=O), 2.34 (t, 12H, N-C<u>H_2</u>-C<u>H_2</u>-N); ^{13}C NMR (100 MHz, DMSO, δ) 165.48, 54.40, 51.80, 43.29, 34.79 ppm; Anal. $C_{18}H_{33}N_6O_3$ (381.0): Calc: C, 56.69; H, 8.66; N, 22.03; found: C, 56.67; H, 8.70; N, 22.04 %.

Synthesis of the polymer Cu(II) complexes [poly-HLCu(II)]: The polymer-metal complexes were prepared according to a reported method[15]. In a 100 mL three-neck round-bottom flask, 2.97 g (0.01 mol) of the polymeric ligand was dissolved in 50/50 mL of ethanol/water; $CuCl_2$ (10 mmol in 15 mL of ethanol) was added and the solution was stirred at 70 °C for 5 h. The solvents were removed under reduced pressure using a rotary evaporator. The reaction mixture was cooled and precipitated into a 75/25 (v/v) diethyl ether/acetone mixture. The coloured precipitate was filtered and then re-precipitated from DMF into methanol. Finally, the product of the polymer-metal complex was dried in a vacuum oven to remove any trapped solvents, which resulted in a blue powder [poly-HLCu(II)] in 70 % yield. FTIR (KBr, ν_{max}, cm^{-1}): 3424, 2925, 2842, 1650, 1435, 1362, 1230, 1105, 825, 750; 530, Anal. $C_{18}H_{31}N_6O_3Cu$ (443.02): Calc. (%): C, 48.80; H, 7.05; N, 18.97; Cu, 14.34; found (%): C, 48.81; H, 7.06; N, 18.95; Cu, 14.36.

Synthesis of the polymer Zn(II) complexes [poly-HLZn(II)]: The poly-HLZn(II) was prepared according to the previously described procedure for the poly-HLCu(II). FTIR ((KBr, ν_{max}, cm^{-1}): 3420, 3250, 2925, 2840, 1650, 1435, 1360, 1232, 1100, 820, 754, 540; ^1H NMR (400 MHz, DMSO, δ): 6.19 (s, 1H, N<u>H</u>), 3.50 (t, 6H, NH-C<u>H_2</u>-C<u>H_2</u>), 2.84 (t, 6H, N-C<u>H_2</u>-CH_2-), 2.40 (t, 6H, -CH_2-C<u>H_2</u>-C=O), 2.30 (t, 12H, N-C<u>H_2</u>-C<u>H_2</u>-N); ^{13}C NMR (100 MHz, DMSO, δ): 171.17, 169.68, 64.59, 62.33, 53.53, 51.58, 35.79 ppm; $C_{18}H_{33}N_6O_3Zn$ (444.88): Calcd. (%): C, 48.60; H, 7.02; N, 18.89; Zn, 14.70; found (%): C, 48.61; H, 7.02; N, 18.90; Zn, 14.72.

Synthesis of the polymer In(III) complexes [poly-LIn(III)]: Poly-LIn(III) was prepared according to the previously described procedure for poly-HLCu(II) and poly-HLZn(II). FTIR (KBr, ν_{max}, cm^{-1}): 2920, 2845, 1650, 1450, 1360, 1232,

1100, 820, 754, 535; Anal. $C_{18}H_{30}N_6O_3In$ (493.28): Calcd. (%): C, 43.83; H, 6.13; N, 17.04; In, 23.28; found (%): C, C, 43.85; H, 6.16; N, 17.08; In, 23.30.

Synthesis of the polymer Ga(III) complexes [poly-LGa(III)]: Poly-LGa(III) was prepared according to a procedure similar to that used for the synthesis of poly-HLCu(II). FTIR (KBr, ν_{max}, cm^{-1}): 2925, 2840, 1655, 1440, 1360, 1230, 1100, 820, 754, 537; Anal. $C_{18}H_{30}N_6O_3Ga$ (44819): Calcd. (%): C, 48.24; H, 6.75; N, 18.75; Ga, 15.56; found (%): C, 48.25; H, 6.76; N, 18.74, Ga, 15.55.

RESULTS AND DISCUSSION

The macrocyclic NOTPA was prepared by the reaction of 1,4,7-triazacyclonoanane (TACN) with acrylic acid at room temperature according to **Scheme-I**. The microanalytical results revealed that the TACN and acrylic acid was in 1:3 molar ratios. A triazamacrocyclic based polymeric ligand was synthesized *via* the polycondensation of NOTPA and ethylenediamine. The polymer-metal complexes were prepared with metal ions (**Scheme-II**). The polymeric ligand and its polymer-metal complexes were soluble in DMF and DMSO but were insoluble in common organic solvents, such as benzene, methanol, ethanol, acetone and water. All of the poly-HLM(II) and polyLM(III) were coloured and obtained in good yield. The elemental analysis of the polymeric ligand indicated that the molar ratio of NOTAP and ethylenediamine was 1:3 and the microanalytical data of the polymer-metal complexes showed that the polymeric ligand and metal chloride were in a 1:1 molar ratio. The molecular weight of poly-H_3L was estimated from GPC (gel permeation chromatography) measurements using THF as a solvent and polystyrene as a standard. The results indicated that the molecular weight was 13,240 Dalton. The molecular weights of the polymer-metal complexes were not determined because of their insolubility in THF. The elemental analysis results indicate that the divalent metal ions Cu(II) and Zn(II) deprotonate only two amide

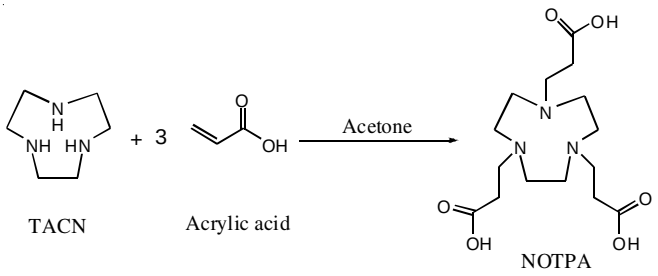

Scheme-I

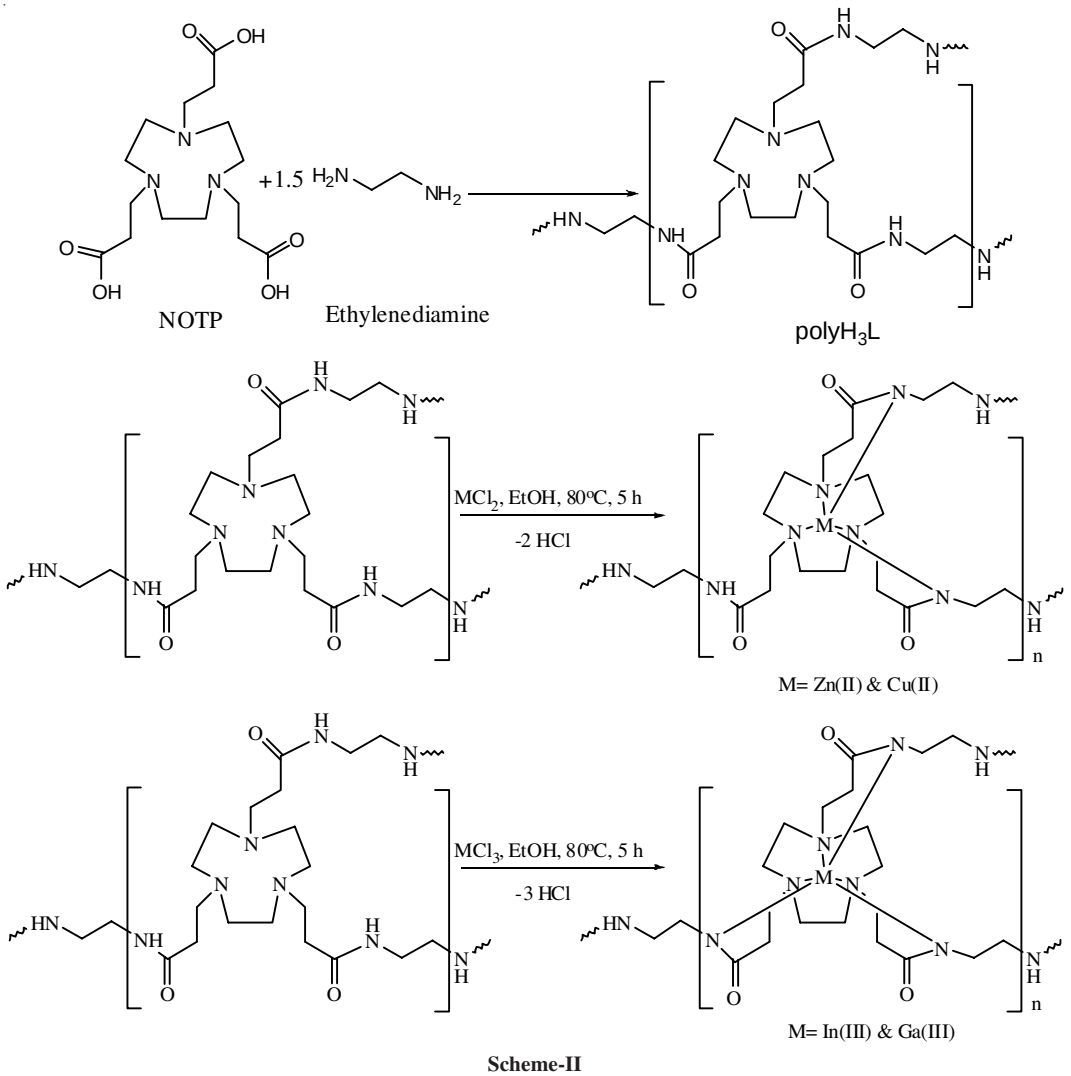

Scheme-II

groups, whereas the trivalent metal ions In(III) and Ga(III) deprotonate all three amide groups on the polymeric ligand. However, slight deviations in the elemental analyses results were observed due to the polymeric nature of the compounds because the end groups of the polymers were not used for the theoretical calculations.

FTIR spectra: The FT-IR spectrum of the polyH_3L displayed a very broad band in the 3425-3270 cm^{-1} region due to asymmetric and symmetric stretching of ν(N-H) (amide groups). The broadening in this region suggests that intermolecular hydrogen bonding occurs[6], possibly between the oxygen and the hydrogen. Two strong bands at 2955-2840 cm^{-1} due to the νCH_2 sym and asym stretching and a band between 1475 and 1460 cm^{-1} due to the CH_2 bending mode were observed[20]. Another band in the 1387-1228 cm^{-1} region is attributed to the C-N stretching. The C=O stretching band of poly-H_3L appears at 1660 cm^{-1}. The poly-HLM(II) show similar spectra with low intensity and less broad band in the 3425-3270 cm^{-1} region due to deprotonation of protons in NH groups. However, in the spectra of poly-LM(III), the NH band disappears because the amide groups are completely deprotonated by the Ga(III) and In(III) ions, The presence of the NH band in the spectra of poly-HLCu(II) and poly-HLZn(II) support the conclusion that these metal complexes are coordinated to three ring and two amide nitrogen atoms, whereas the poly-LIn(III) and poly-LGa(III) metal complexes are coordinated to three ring and three amide nitrogen atoms. The formation of poly-HLM(II) and poly-LM(III) is further supported by the appearance of M-N stretching vibrations[21] between 530 and 545 cm^{-1}.

^{1}H NMR and ^{13}C NMR spectra: The ^{1}H NMR spectra of poly-H_3L and poly-HLZn(II) were determined in DMSO-d_6 and shown in Fig. 1. The resonance signals of amide group, CH_2-NH signals appear at 8.14 in the spectra of poly-H_3L, which had actually shifted downfield from its original position because of the intermolecular and intramolecular hydrogen bonding between the NH and C=O groups. The resonance signal at 8.14 ppm in the spectra of poly-HLZn(II) is low intense due to deprotonation or two protons with meta ions[22]. The presence of methylene group in different environment of poly-H_3L and poly-HLZn(II) show resonance signal at 2.45-2.34 ppm, other resonance signals of the ring appear at 3.35 and 2.84 ppm, which may be due to the presence of CH_2 protons in different environments.

In the ^{13}C NMR spectra of poly-H_3L and poly-HLZn(II) are shown in Fig. 2, the signals for the CH_2 groups of appear at 54.40, 51.80, 43.29 and 34.79 ppm. The C=O resonance signal appears at 165.48 ppm[23]. The resonance signal of the carbonyl group in poly-HLZn(II) appears at 164.62 and 160.10 ppm because the carbonyl carbon occurs in two different environments due to the deprotonation of two NH groups. Other CH_2 resonance peaks appear at 54.50, 52.34, 44.52, 40.55 and 35.60 ppm. It is also observed that the solvent (DMSO) did not produce any coordinating effects in the ^{1}H NMR and ^{13}C NMR spectra.

UV-visible spectra of poly-LH_3, poly-HLM(II) and poly-LM(III): The electronic spectra of polymeric ligand and its polymer metal complexes were recorded in DMSO and are shown in Fig. 3. For the polymeric ligand, the absorption bands

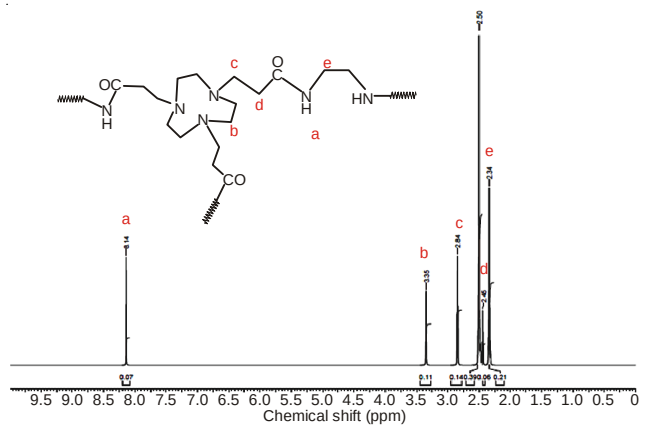

Fig. 1. ^{1}H NMR spectra of poly-H_3L

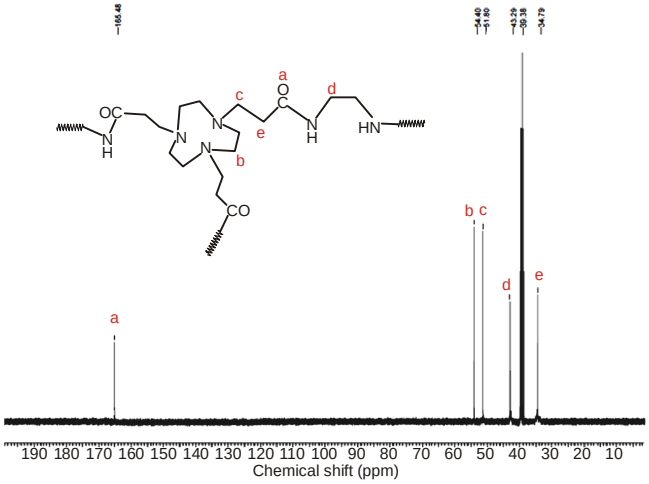

Fig. 2. ^{13}C NMR spectra of poly-H_3L

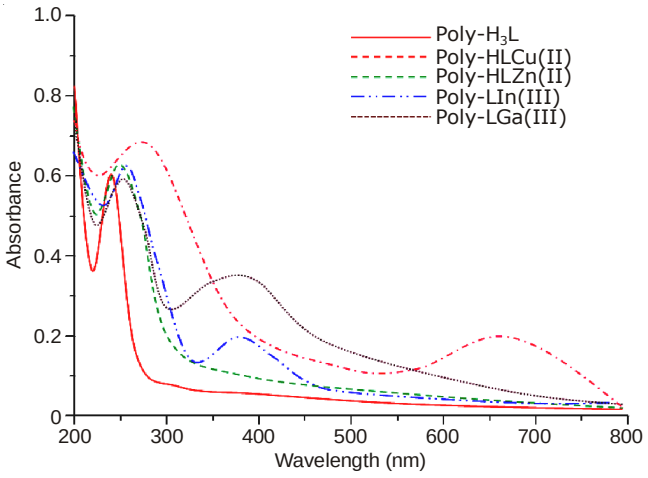

Fig. 3. Electronic spectra of poly-H_3L, poly-HLM(II) and poly-LM(III)

at 240 nm can be attributed to the n → π* electronic transition. The electronic spectra of the polymeric ligands differed from that of the free ligand within the visible region of 400-800 nm. The spectrum of poly-HLCu(II) exhibits an absorption maximum at 684 cm^{-1} with an extinction coefficient of 50 M^{-1} due to the *d-d* transition in the Cu(II) ions (d^9) with a tetragonal Jahn-Teller distortion[24]. The cyclic nature of the polymeric ligand limits the extent of this distortion and the difference between the axial and equatorial bond lengths compared to those observed with noncyclic ligand-Cu(II) complexes. This

structure exhibited a higher level of distortion, which resulted in one protonated amide group that was not coordinated to the metal center. Poly-HLCu(II) was assigned as a five-coordinate complex and exhibited a square-pyramidal geometry around the Cu(II) ions. The spectra of poly-LIn(III) and poly-LGa(III) showed absorption bands in the visible region at 385 and 390 nm, respectively, which correspond to a distorted octahedral geometry[25]. The electronic spectra of poly-HLZn(II) did not show any absorption bands in the visible region due to the absence of unpaired *d* electrons (d^{10}).

ESR spectra: The ESR spectrum of poly-HLCu(II) is shown in Fig. 4 and anisotropic with a resolved hyperfine structure and has g^{II} (2.360) and $g^{\perp}$ (2.114) values greater than 2.04, which is consistent with a distorted square-pyramidal geometry around the Cu(II) ions with all of the principle axes aligned parallel. These values indicate that the unpaired *d*-electron is in the $d_{x^2-y^2}$ orbital and the spectral features are characteristic of axial symmetry. The *g*-values can be used to calculate the G value, which indicates whether the ligand is weak-field or strong-field. The equation used to calculate the G value is $G = (g^{II}-2.002)/(g^{\perp}-2.002)$. If the G value is less than 4.0, the ligand forming the Cu(II) complex is a strong-field ligand[26,27]. In the case of poly-HLCu(II), the G value was 3.19, which indicates the formation of a strong-field ligand.

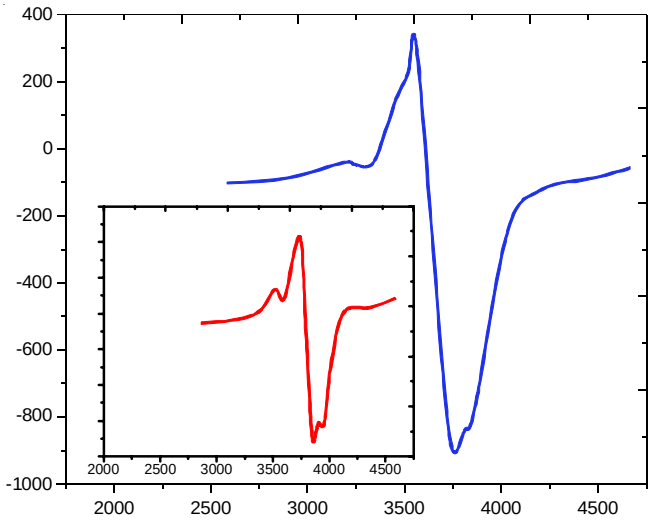

Fig. 4. ESR spectrum of poly-HLCu(II)

Thermal analyses and thermal kinetics: The TGA and DTA curves of polymeric ligand and its metal complexes are shown in Fig. 5 and 6, respectively. The thermal degradation of polymeric ligand is divided into four stages: the first is the drying stage and corresponds to the removal of absorbed solvents and humidity (< 150 °C); the second is the degradation stage between 150-312 °C, the third is the main degradation stage and it occurs between 312 and 500 °C; and the last is the carbonization stage (> 500 °C). An initial 6.133 % weight loss was observed at 150 °C for poly-H_3L. However, for the poly-HLM(II) and poly-LM(III) complexes, only a 4.69-5.50 % weight loss was observed, which indicates that no water molecules are coordinated to the polymer-metal complexes. In the second stage, approximately 13.94 % of the weight was observed up to 312 °C for poly-H_3L; the third is the main degradation

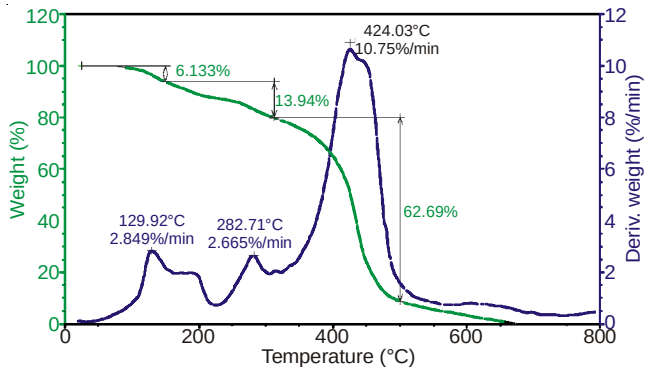

Fig. 5. Thermogravimetric analysis (TGA) and differential thermal analysis (DTA) curves of poly-H_3L

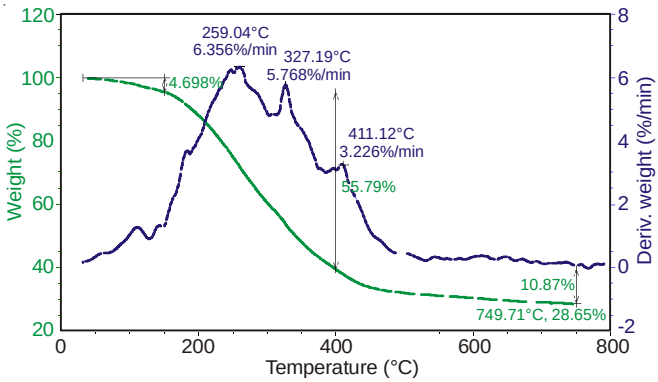

Fig. 6. Thermogravimetric analysis (TGA) and differential thermal analysis (DTA) curves of poly-HLCu(II)

stage, in this stage 62.69 % weigh loss occurs between 312 and 500 °C; the ligand was completely decomposed into volatile products at 650 °C. However, the polymer-metal complexes are not completely decomposed even at 750 °C. The results of the thermogravimetric analysis revealed that poly-HLCu(II) is more thermally stable than the other polymer-metal complexes. The thermal stability of poly-HLCu(II) is greater than the others because the Cu(II) ions have a greater stability constant. The order of stability on the basis of thermal residual weight at 750 °C was poly-HLCu(II) > poly-HLZn(II) > poly-LIn(III) > poly-LGa(III) and the residual weight was 28.65, 26.22, 26.80 and 24.24 %, respectively.

The DTG curve (*i.e.*, the mass-loss rate) of poly-H_3L during the degradation was used to calculate the kinetic parameters. The maximum mass loss rates were 10.758 % min^{-1} at 424.97 °C.

The first-order reaction based on Arrhenius's theory is commonly assumed in the kinetic analysis of pyrolysis (eqn. 1)[28]:

$$k = A\exp\left(-\frac{E}{RT}\right) \quad (1)$$

where k is the reaction rate constant, T is the thermodynamic temperature, R is the universal gas constant, E is the activation energy and A is a pre-exponential factor.

The integration function utilized is shown below.

$$g(\alpha) = \int_0^{\alpha}\frac{d\alpha}{dt} = \frac{A}{\beta}\int_0^{t}\exp\left(-\frac{E}{RT}\right)dT \quad (2)$$

where $g(\alpha) = -\ln(1-\alpha)$. Eqn. 2 is integrated using the Coats-Redfern method:

$$\ln\frac{g(\alpha)}{T^2} = \ln\left(\frac{AR}{\beta E}\left[1-\frac{2RT}{E}\right]\right) - \frac{E}{RT} \quad (3)$$

where g(α) is the kinetic mechanism function in integral form.

The 2RT/E term can be neglected because it is much less than 1 and eqn. 3 can be simplified to

$$\ln\frac{g(\alpha)}{T^2} = \ln\left(\frac{AR}{\beta E}\right) - \frac{E_1}{RT} \quad (4)$$

The $\ln[g(\alpha)/T^2]$ term varies linearly with 1/T at a slope of -E/R and the y-axis intercept of the line is related to the pre-exponential factor A. Both the activation energy E and pre-exponential factor A can be determined from the slope and intercept of the line and are presented in Table-1. We observed that the activation energy of poly-LGa(III) is slightly greater than those of the other metal complexes as shown in Fig. 7.

Biological assays: The antibacterial activity of poly-H_3L, poly-HLM(II) and poly-LM(III) was studied against several bacteria and the results are summarized in Table-2. Poly-H_3L show zone of inhibition values, *i.e*. 12, 14 and 15 mm against *S. aureus*, *S. typhi* and *B. subtilis,* respectively. Poly-LIn(III) show zone of inhibition values, *i.e*.16, 18 and 18 mm were measured against *S. typhi*, *B. subtilis* and *E. coli* , respectively.

TABLE-1
THERMAL KINETIC PARAMETERS AND RESIDUE WEIGHT AT 750 °C
OF POLY-H_3L AND ITS POLYMER METAL COMPLEXES

Abbreviations	Weight loss rate/temperature (°C)	Activation energy (J mol^{-1})	Pre-exponential factor	R^2	Percentage weight at 750 °C (%)
Poly-H_3L	10.75 % min^{-1} at 424 °C	1.79×10^{-4}	3.96E + 00	0.976	-
Poly-HLCu(II)	3.22 % min^{-1} at 411.12 °C	2.01×10^{-4}	4.12E + 01	0.978	28.65
Poly-HLZn(II)	3.56 % min^{-1} at 407.36 °C	2.08×10^{-4}	4.46 E + 02	0.962	26.22
Poly-LIn(III)	4.21 % min^{-1} at 402.36 °C	2.01×10^{-4}	4.28E + 00	0.974	26.80
Poly-LGa(III)	4.58 % min^{-1} at 400.68 °C	2.23×10^{-4}	4.32E + 01	0.978	24.24

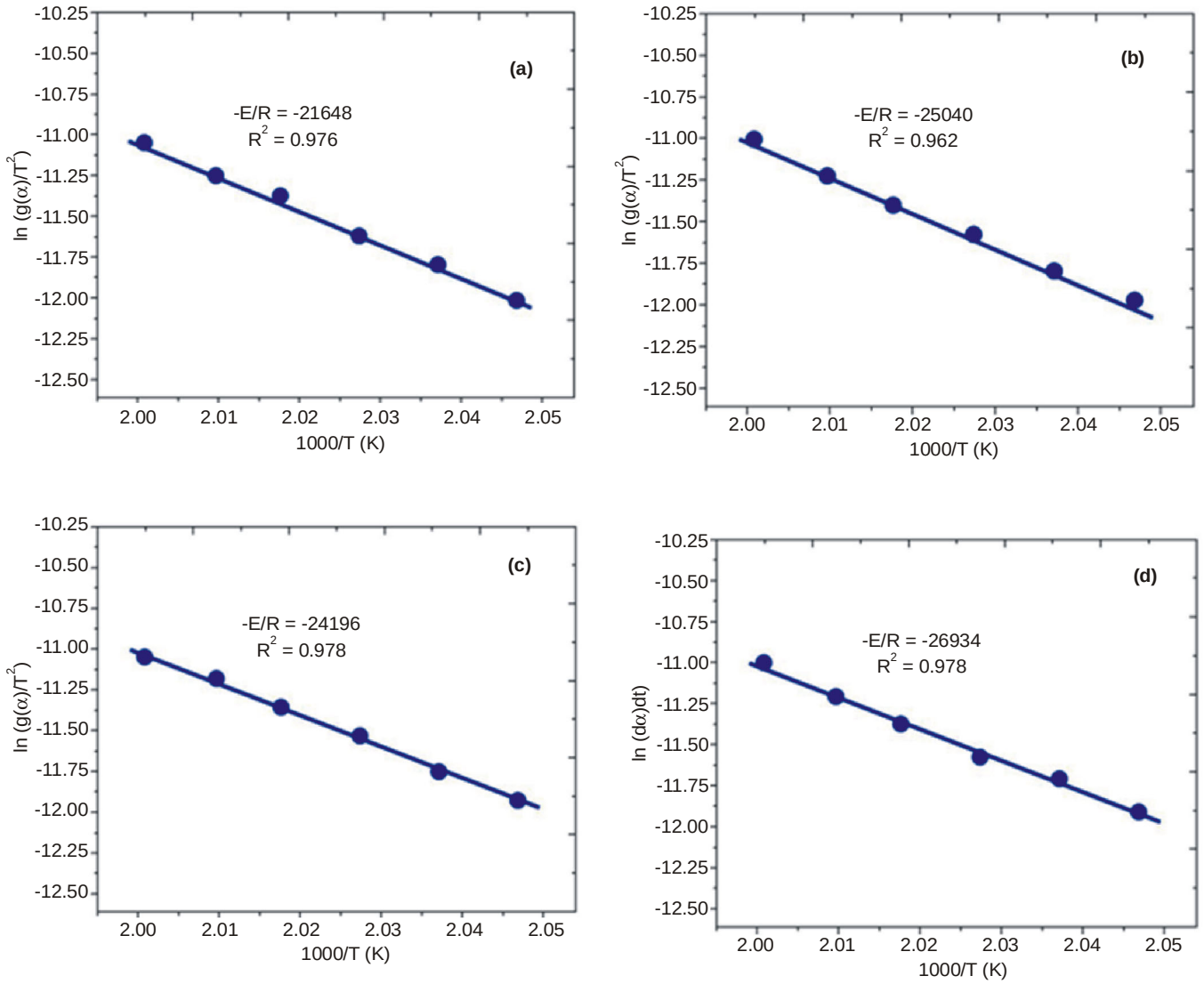

Fig. 7. Coast-Redfern model plot (a) poly-H_3L (b) poly-HLZn (c) poly-HLCu(II) (d) poly-LGa(III)

TABLE-2
ANTIBACTERIAL ACTIVITY OF POLY-H_3L, POLY-HLM(II) AND POLY-LM(III)

Abbreviations	Zone of inhibition[a] (mm) 50 µg/disk					
	B. subtilis	*B. megaterium*	*S. aureus*	*E. coli*	*P. aeruginosa*	*S. typhi*
Poly-H_3L	15	14	12	15	14	14
Poly-HLCu(II)	17	17	19	17	17	20
Poly-HLZn(II)	18	16	17	16	18	17
Poly-LIn(III)	18	15	14	18	17	16
Poly-LGa(III)	19	16	16	17	20	16
Kanamycin[b]	29	29	27	29	30	29
DMSO[c]	-	-	-	-	-	-

[a]18-30 mm = significantly active; 10-17 mm moderately active; < 10 mm = weakly active; [b]Standard drug (positive control); [c]Solvent (negative control)

TABLE-3
ANTIFUNGAL ACTIVITY OF POLY-H_3L, POLY-HLM(II) AND POLY-LM(III)

Abbreviations	Zone of inhibition[a] (mm) 100 µg/disk					
	C. albicans	*T. species*	*A. flavus*	*A. niger*	*F. species*	*M. species*
Poly-H_3L	14	15	16	15	15	16
Poly-HLCu(II)	18	22	20	18	16	19
Poly-HLZn(II)	16	17	18	17	16	18
Poly-LIn(III)	18	16	14	16	17	18
Poly-LGa(III)	16	18	16	18	16	19
Miconazole[b]	22	25	25	25	25	25
DMSO[c]	-	-	-	-	-	-

[a]18-30 mm = significantly active; 10-17 mm moderately active; < 10 mm = weakly active; [b]Standard drug (positive control); [c]Solvent (negative control)

The poly-HLCu(II) show highest inhibition zone values, *i.e.* 20 against *S. typhi*. Poly-LGa(III) show zone of inhibition values, *i.e.* 16, 19 and 20 mm were measured against, *S. aureus*, *B. subtilis* and *P. aeruginosa*, respectively. The results of antibacterial activities revealed that the poly-HLM(II) and poly-LM(III) show higher zone of inhibition than poly-H_3L due to the coordination of metal ions. Comparison with a standard drug, kanamycin (30 µg), showed that the inhibition effect of the polymer metal complexes on bacterial growth was significantly active.

The antifungal activity of poly-H_3L and its polymer-metal complexes was studied and the results are presented in Table-3. The polymeric ligand showed zone-of-inhibition values of 15, 15 and 14 mm against *A. flavus*, *A. niger* and *M. species*, respectively. Poly-HLZn(II) displayed promising zone of inhibition values of 14, 14 and 16 mm against *T. species*, *A. niger* and *M. species*, respectively, whereas poly-LIn(III) showed zone-of-inhibition values of 15 and 14 mm against *F. species* and *M. species*, respectively. Poly-HLCu(II) demonstrated promising zone of inhibition values of 16, 18 and 17 mm against *M. species*, *A. flavus* and *A. niger*, respectively. This investigation revealed that the antimicrobial activity of the compounds increased after metal chelation. This effect was observed because chelation reduces the polarity of the central metal ion through partial sharing of its positive charge with the donor groups[29]. This process increases the lipophilic nature of the central metal ion, which, in turn, favors its permeation to the lipid layer of the membrane[20].

Conclusion

A new polymeric ligand (poly-H_3L) was synthesized *via* polycondensation of NOTA with ethylenediamine in a 1:3 molar ratio. The results of the elemental and spectral analyses revealed that poly-HLCu(II) and poly-HLZn(II) are five-coordinate complexes and that the metals are coordinated to the three ring nitrogen atoms and coordinate covalently bonded to the two amide groups. In contrast, poly-LIn(III) and poly-LGa(III) are six-coordinate complexes due to coordination of the metals to the three ring nitrogen atoms and deprotonation of all three amide groups. All of the synthesized polymers demonstrated excellent antimicrobial activity against several bacteria and fungi. The results of the biological evaluation indicate that poly-HLM(II) exhibited greater antimicrobial activity than the poly-H_3L. Because these polymers show promising antibacterial and antifungal activity against several microbes, they may be useful in future medical and biomaterial applications.

ACKNOWLEDGEMENTS

This work was supported by the Deanship for Scientific Research, Research Center, College of Science, King Saud University, Riyadh.

REFERENCES

1. A.B. Abibe, S.T. Amancio-Filho, J.F. dos Santos and E. Hage Jr., *Mater. Des.*, **46**, 338 (2013).
2. T. Ahamad and S.M. Alshehri, *Polym. Int.*, **61**, 1640 (2012).
3. T. Ahamad and S.M. Alshehri, *Spectrochim. Acta A*, **96**, 179 (2012).
4. T. Ahamad and S.M. Alshehri, *J. Coat. Technol. Res.*, **9**, 515 (2012).
5. T. Ahamad and S.M. Alshehri, *Spectrochim. Acta A*, **108**, 26 (2013).
6. T. Ahamad, V. Kumar and N. Nishat, *J. Biomed. Mater. Res. A*, **88**, 288 (2009).
7. T. Ahamad, V. Kumar, S. Parveen and N. Nishat, *Appl. Organomet. Chem.*, **21**, 1013 (2007).
8. T. Ahamad and N. Nishat, *J. Appl. Polym. Sci.*, **107**, 2280 (2008).
9. N. Nishat, T. Ahamad, M. Zulfequar and S. Hasnain, *J. Appl. Polym. Sci.*, **110**, 3305 (2008).

10. C.L. Ferreira, D.T.T. Yapp, D. Mandel, R.K. Gill, E. Boros, M.Q. Wong, P. Jurek and G.E. Kiefer, *Bioconjug. Chem.*, **23**, 2239 (2012).
11. C. Förster, M. Schubert, H.J. Pietzsch and J. Steinbach, *Molecules*, **16**, 5228 (2011).
12. J. Gao, N. Wang, X. Xiong, C. Chen, W. Xie, X. Ran, Y. Long, S. Yue and Y. Liu, *CrystEngComm*, **15**, 3261 (2013).
13. H. Hong, Y. Zhang, H. Orbay, H.F. Valdovinos, T.R. Nayak, J. Bean, C.P. Theuer, T.E. Barnhart and W. Cai, *Mol. Pharm.*, **10**, 709 (2013).
14. A. Kiviniemi, J. Mäkel, J. Mäkil, T. Saanijoki, H. Liljenbäck, P. Poijärvi-Virta, H. Lönnberg, T. Laitala-Leinonen, A. Roivainen and P. Virta, *Bioconjug. Chem.*, **23**, 1981 (2012).
15. J. Notni, K. Pohle, H.J. Wester, *EJNMMI Res.*, **2** (2012).
16. J. Šimeèek, P. Hermann, H.J. Wester and J. Notni, *Chem. Med. Chem*, **8**, 95 (2013).
17. J. Šimeèek, M. Schulz, J. Notni, J. Plutnar, V. Kubíèek, J. Havlíèková and P. Hermann, *Inorg. Chem.*, **51**, 577 (2012).
18. K. Suzuki, M. Satake, J. Suwada, S. Oshikiri, H. Ashino, H. Dozono, A. Hino, H. Kasahara and T. Minamizawa, *Nucl. Med. Biol.*, **38**, 1011 (2011).
19. J.F. Desreux, *Inorg. Chem.*, **19**, 1319 (1980).
20. N. Nishat, T. Ahamad, S. Ahmad and S. Parveen, *J. Coord. Chem.*, **64**, 2639 (2011).
21. N. Nishat, T. Ahamad, S.M. Alshehri and S. Parveen, *Eur. J. Med. Chem.*, **45**, 1287 (2010).
22. P.F. Kelly, A.M.Z. Slawin and A. Soriano-Rama, *J. Chem. Soc., Dalton Trans.*, **1**, 53 (1996).
23. I.H. Hall, S.Y. Chen, B.J. Barnes and D.X. West, *Met. Based Drugs*, **6**, 143 (1999).
24. A.B.P. Lever, Inorganic Electronic Spectroscopy, Elsevier, Amsterdam, The Netherlands, p. 420 (1968).
25. E. Cole, R.C.B. Copley, J.A.K. Howard, D. Parker, G. Ferguson, J.F. Gallagher, B. Kaitner, A. Harrison and L. Royle, *J. Chem. Soc., Dalton Trans.*, 1619 (1994).
26. D. Kivelson and R. Neiman, *J. Chem. Phys.*, **35**, 149 (1961).
27. K. Narang and V. Singh, *Transition Met. Chem.*, **21**, 5079 (1996).
28. H. Pan, T.F. Shupe and C.Y. Hse, *J. Appl. Polym. Sci.*, **108**, 1837 (2008).
29. R.S. Bottei and J.T. Fangman, *J. Inorg. Nucl. Chem.*, **28**, 1259 (1966).